A Short Hike Through Symbolic Dynamics

And the Random Noise Therein

Léo Gayral

03/05/2022, Séminaire de probabilités de l'institut Fourier

Joint work with Mathieu Sablik
IMT, Université Toulouse III Paul Sabatier

Folklore on Symbolic Dynamics

Subshifts of Finity Type (SFTs)

Symbolic Dynamics on Groups

Dynamical System:

- Phase Space Ω,
- Operators $(f_k : \Omega \to \Omega)$.

$\Longrightarrow$

Symbolic Dynamics:

- Group G with generators (a_k),
- Finite Alphabet $\mathcal{A}$,
- Phase Space $\Omega = \mathcal{A}^G$,
- Shift Operators σ_k,
  s.t. $\sigma_k(\omega)_g = \omega_{-a_k+g}$.

Subshifts of Finite Type and Forbidden Patterns

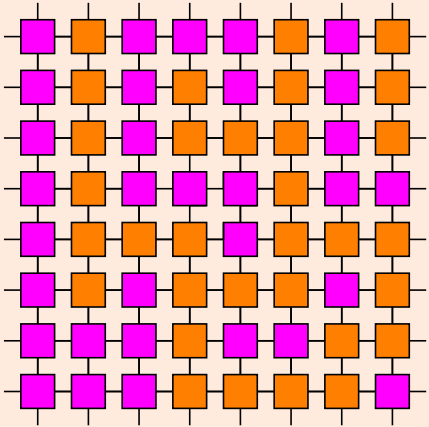

Figure 1: Example of configuration,

- Group $G = \mathbb{Z}^2$ with 2 generators.
- Alphabet $\mathcal{A} = \{$ ■, ■ $\}$.

Subshifts of Finite Type and Forbidden Patterns

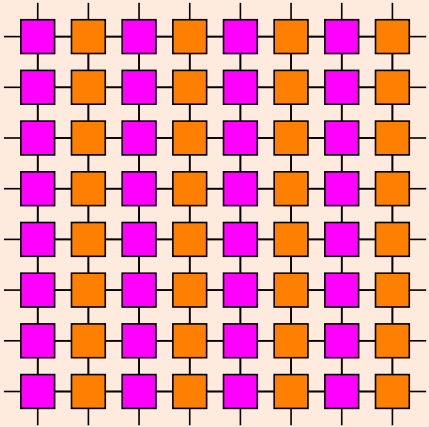

Figure 1: Example of configuration, without occurrences of the forbidden patterns.

- Group $G = \mathbb{Z}^2$ with 2 generators.
- Alphabet $\mathcal{A} = \{$ ■, ■ $\}$.
- Finite set of forbidden patterns $\mathcal{F}$:

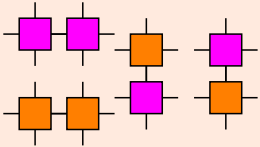

Subshifts of Finite Type and Forbidden Patterns

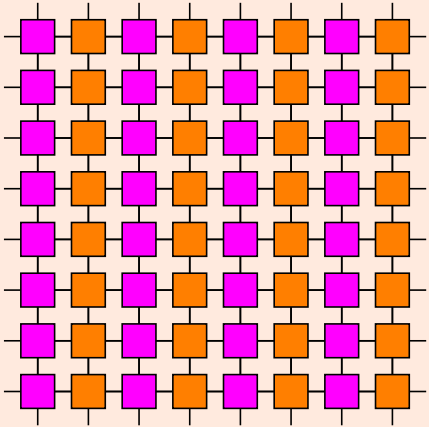

Figure 1: Example of configuration, without occurrences of the forbidden patterns.

- Group $G = \mathbb{Z}^2$ with 2 generators.
- Alphabet $\mathcal{A} = \{\blacksquare, \blacksquare\}$.
- Finite set of forbidden patterns $\mathcal{F}$:

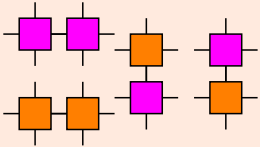

- The SFT is the space $\Omega_{\mathcal{F}} \subset \mathcal{A}^G$ of such configurations.

Why SFTs?

- Continuous Dynamical Systems:
  - Represent orbits through a finite/countable amount of information.
- Statistical Physics:
  - Ising model,
  - Domino models,
  - Quasicrystal models.
- Information Theory:
  - Space-time diagrams of cellullar automata,
  - Computing model encoding Turing machines with a geometrical structure.

Folklore on Symbolic Dynamics

(A)periodicity

Periodic SFT

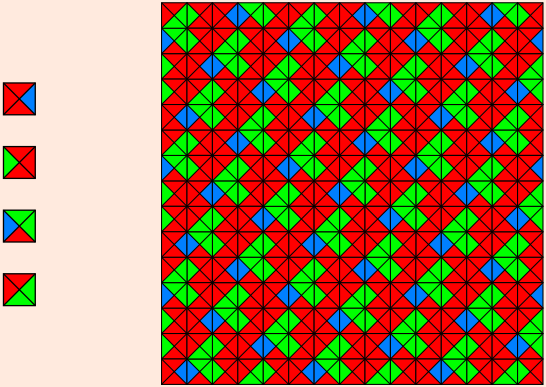

Figure 2: A periodic configuration,

Periodic SFT

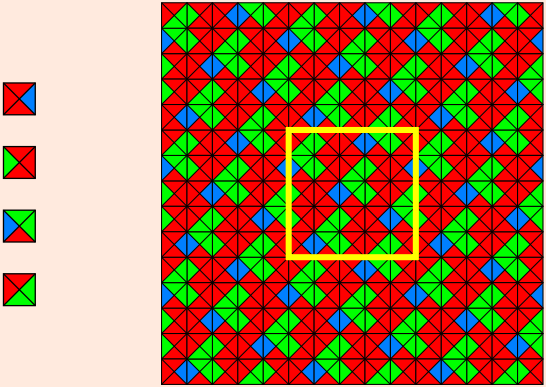

Figure 2: A periodic configuration, characterised by a base hypercube that repeats in all directions.

Aperiodic SFT

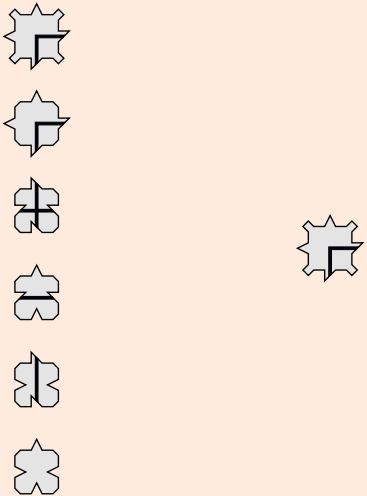

Figure 3: Hierarchical structure of the Robinson tiling.

Aperiodic SFT

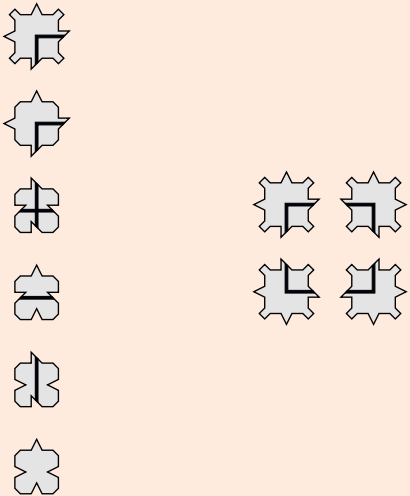

Figure 3: Hierarchical structure of the Robinson tiling.

Aperiodic SFT

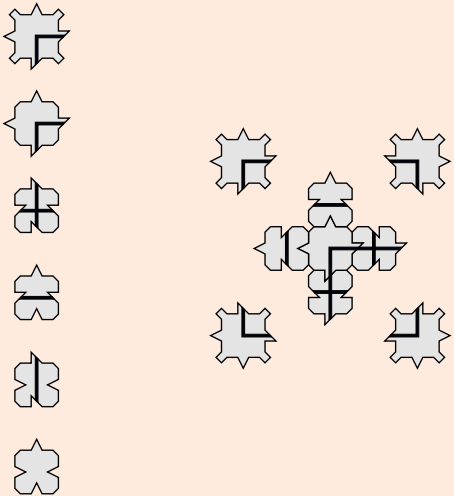

Figure 3: Hierarchical structure of the Robinson tiling.

Aperiodic SFT

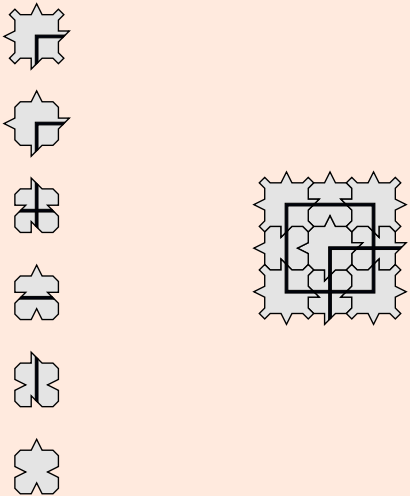

Figure 3: Hierarchical structure of the Robinson tiling.

Aperiodic SFT

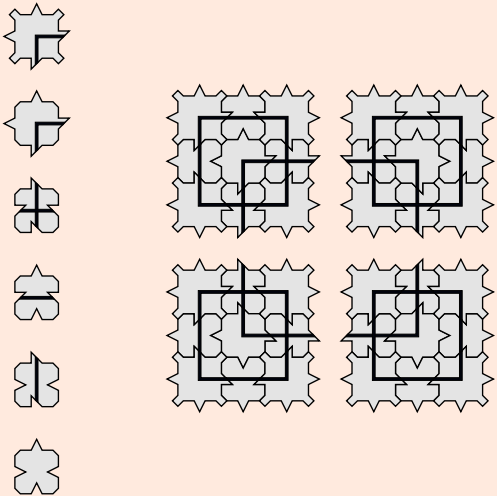

Figure 3: Hierarchical structure of the Robinson tiling.

Aperiodic SFT

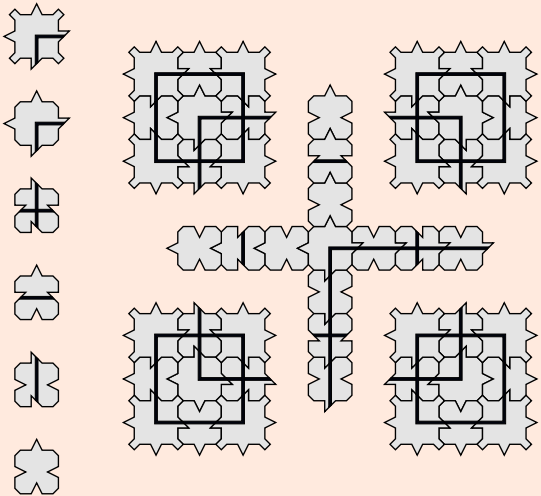

Figure 3: Hierarchical structure of the Robinson tiling.

Aperiodic SFT

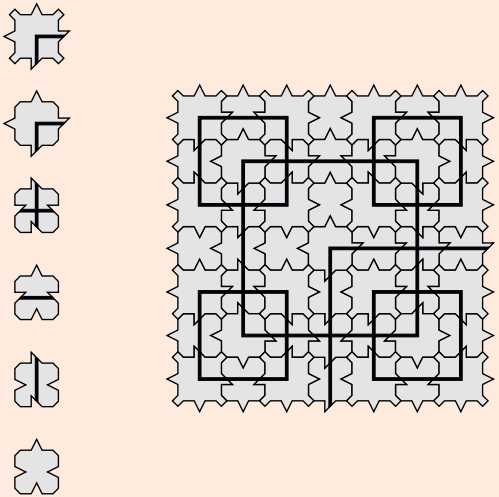

Figure 3: Hierarchical structure of the Robinson tiling.

Liminal Cases

Consider the following Diluted Domino tiling:

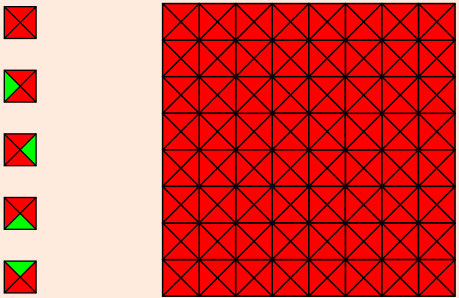

Figure 4: This tileset forces no specific behaviour on admissible configurations.

Liminal Cases

Consider the following Diluted Domino tiling:

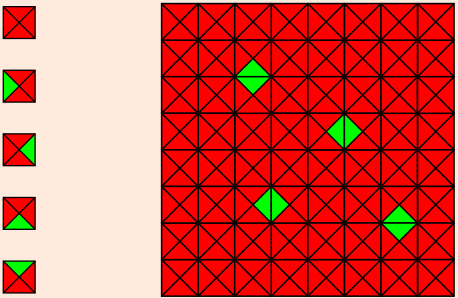

Figure 4: This tileset forces no specific behaviour on admissible configurations.

Folklore on Symbolic Dynamics

From Configurations to Measures

Onto Ergodic Theory

Denote $\mathcal{M}_{\mathcal{F}}$ the σ-invariant measures on $\Omega_{\mathcal{F}}$, such that $\sigma_k^*(\mu) = \mu$ for any k.

Usual Ergodic Theory results, such as Birkhoff's pointwise convergence theorem, naturally extend to this d-dimensional setting.

What About Noise?

There are several ways of adding noise to tilings.

- Statistical Physics Viewpoint: Gibbs Measures

Theorem [Fernique, Gayral and Sablik]

Denote T the number of cycles around a vertex.

Consider the Gibbs measure $\mu_\beta(\omega) = \frac{1}{Z} e^{-\beta E(\omega)}$,
with E the number of forbidden interfaces in ω.

We have $\mathbb{E}_\beta[T] \leq \exp\left(\frac{9e^{2\beta}}{2(e^\beta+2)^2} \times \frac{1}{(e^\beta-2)^2}\right) - 1 < \infty$ when $\beta > \ln(2)$.

What About Noise?

There are several ways of adding noise to tilings.

- Statistical Physics Viewpoint: Gibbs Measures

Theorem [Fernique, Gayral and Sablik]

Denote T the number of cycles around a vertex.

Consider the Gibbs measure $\mu_\beta(\omega) = \frac{1}{Z} e^{-\beta E(\omega)}$, with E the number of forbidden interfaces in ω.

We have $\mathbb{E}_\beta[T] \leq \exp\left(\frac{9e^{2\beta}}{2(e^\beta+2)^2} \times \frac{1}{(e^\beta-2)^2}\right) - 1 < \infty$ when $\beta > \ln(2)$.

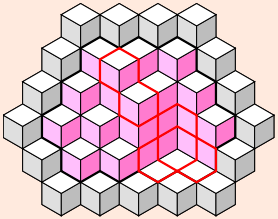

Figure 5: Dimer tiling on the triangle lattice, with forbidden interfaces.

What About Noise?

There are several ways of adding noise to tilings.

- Statistical Physics Viewpoint: Gibbs Measures

Theorem [Fernique, Gayral and Sablik]

Denote T the number of cycles around a vertex.

Consider the Gibbs measure $\mu_\beta(\omega) = \frac{1}{Z} e^{-\beta E(\omega)}$,
with E the number of forbidden interfaces in ω.

We have $\mathbb{E}_\beta[T] \leq \exp\left(\frac{9e^{2\beta}}{2(e^\beta+2)^2} \times \frac{1}{(e^\beta-2)^2}\right) - 1 < \infty$ when $\beta > \ln(2)$.

- Information Theory Viewpoint: Bernoulli Noise

Moving onto Noisy Tilings

Clair-Obscur Framework

- Inject $\mathcal{A} \hookrightarrow \widetilde{\mathcal{A}} = \mathcal{A} \times \{0, 1\}$.
- Identify $\mathcal{F} \cong \widetilde{\mathcal{F}} = \mathcal{F} \times \{0\}$.
- Denote $\widetilde{\mathcal{M}_{\mathcal{F}}^{\mathcal{B}}}(\varepsilon) \subset \mathcal{M}_{\widetilde{\mathcal{F}}}$ the measures with $\mathcal{B}(\varepsilon)^{\otimes \mathbb{Z}^d}$ Bernoulli noise.
- The set $\widetilde{\mathcal{M}_{\mathcal{F}}^{\mathcal{B}}}(\varepsilon)$ is weak-* closed, and $\bigcap_{\varepsilon > 0} \widetilde{\mathcal{M}_{\mathcal{F}}^{\mathcal{B}}}(\varepsilon) \approx \mathcal{M}_{\mathcal{F}}$.

×	○	×	○	×	○	×	○	×	○	×	○	×
○	○	×	○	○	×	×	○	×	○	×	○	×
×	○	○	○	○	○	×	×	○	○	×	○	×
○	×	×	×	○	×	○	×	○	×	○	×	○
×	○	×	×	×	×	○	○	○	○	○	○	×
○	○	×	×	×	×	○	×	○	○	×	○	×
×	×	×	○	×	○	○	×	×	○	○	○	×
○	×	○	×	○	×	×	×	×	×	○	×	○

Figure 6: Chequerboard,

Clair-Obscur Framework

- Inject $\mathcal{A} \hookrightarrow \widetilde{\mathcal{A}} = \mathcal{A} \times \{0, 1\}$.
- Identify $\mathcal{F} \cong \widetilde{\mathcal{F}} = \mathcal{F} \times \{0\}$.
- Denote $\widetilde{\mathcal{M}_{\mathcal{F}}^{\mathcal{B}}}(\varepsilon) \subset \mathcal{M}_{\widetilde{\mathcal{F}}}$ the measures with $\mathcal{B}(\varepsilon)^{\otimes \mathbb{Z}^d}$ Bernoulli noise.
- The set $\widetilde{\mathcal{M}_{\mathcal{F}}^{\mathcal{B}}}(\varepsilon)$ is weak-* closed, and $\bigcap_{\varepsilon > 0} \widetilde{\mathcal{M}_{\mathcal{F}}^{\mathcal{B}}}(\varepsilon) \approx \mathcal{M}_{\mathcal{F}}$.

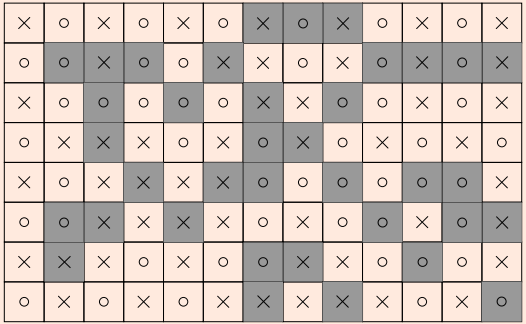

Figure 6: Chequerboard, now with obscured cells.

Clair-Obscur Framework

- Inject $\mathcal{A} \hookrightarrow \widetilde{\mathcal{A}} = \mathcal{A} \times \{0, 1\}$.
- Identify $\mathcal{F} \cong \widetilde{\mathcal{F}} = \mathcal{F} \times \{0\}$.
- Denote $\widetilde{\mathcal{M}_{\mathcal{F}}^{\mathcal{B}}}(\varepsilon) \subset \mathcal{M}_{\widetilde{\mathcal{F}}}$ the measures with $\mathcal{B}(\varepsilon)^{\otimes \mathbb{Z}^d}$ Bernoulli noise.
- The set $\widetilde{\mathcal{M}_{\mathcal{F}}^{\mathcal{B}}}(\varepsilon)$ is weak-* closed, and $\bigcap_{\varepsilon > 0} \widetilde{\mathcal{M}_{\mathcal{F}}^{\mathcal{B}}}(\varepsilon) \approx \mathcal{M}_{\mathcal{F}}$.

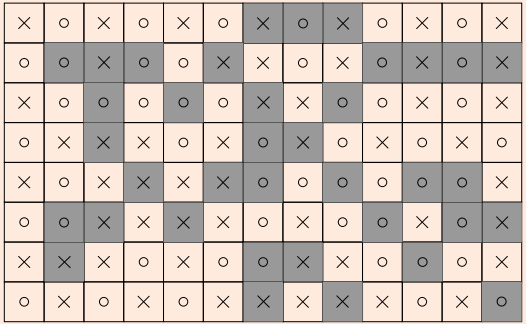

Figure 6: Chequerboard, now with obscured cells.

Clair-Obscur Framework

- Inject $\mathcal{A} \hookrightarrow \widetilde{\mathcal{A}} = \mathcal{A} \times \{0, 1\}$.
- Identify $\mathcal{F} \cong \widetilde{\mathcal{F}} = \mathcal{F} \times \{0\}$.
- Denote $\widetilde{\mathcal{M}_{\mathcal{F}}^{\mathcal{B}}}(\varepsilon) \subset \mathcal{M}_{\widetilde{\mathcal{F}}}$ the measures with $\mathcal{B}(\varepsilon)^{\otimes \mathbb{Z}^d}$ Bernoulli noise.
- The set $\widetilde{\mathcal{M}_{\mathcal{F}}^{\mathcal{B}}}(\varepsilon)$ is weak-* closed, and $\bigcap_{\varepsilon > 0} \widetilde{\mathcal{M}_{\mathcal{F}}^{\mathcal{B}}}(\varepsilon) \approx \mathcal{M}_{\mathcal{F}}$.

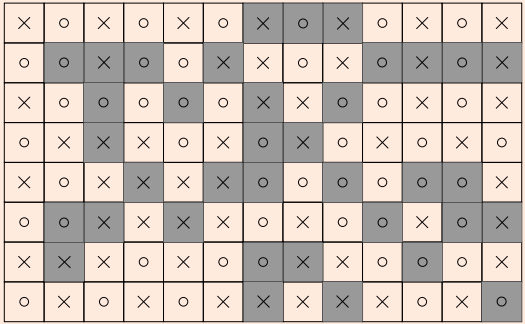

Figure 6: Chequerboard, now with obscured cells.

Reminder (Weak-* Convergence)

We say that $\mu_n \xrightarrow{*} \mu$ when $\mu_n([w]) \to \mu([w])$ for any finite pattern w.

Besicovitch Distance

x

×	○	×	○	×	○	×	○	×	○	×	○	×
○	○	×	○	○	×	×	○	×	○	×	○	×
×	○	○	○	○	○	×	×	○	○	×	○	×
○	×	×	×	○	×	○	×	○	×	○	×	○
×	○	×	×	×	×	○	○	○	○	○	○	×
○	○	×	×	×	×	○	×	○	○	×	○	×
×	×	×	○	×	○	○	×	×	○	○	○	×
○	×	○	×	○	×	×	×	×	×	○	×	○

Figure 7: Frequency of differences between x and y.

Finite Hamming distance:

$d_{13\times 8}(x, \quad) = \frac{\quad}{13\times 8}$

Besicovitch Distance

y

×	○	×	○	×	○	×	○	×	○	×	○	×
○	×	○	×	○	×	○	×	○	×	○	×	○
×	○	×	○	×	○	×	○	×	○	×	○	×
○	×	○	×	○	×	○	×	○	×	○	×	○
×	○	×	○	×	○	×	○	×	○	×	○	×
○	×	○	×	○	×	○	×	○	×	○	×	○
×	○	×	○	×	○	×	○	×	○	×	○	×
○	×	○	×	○	×	○	×	○	×	○	×	○

Figure 7: Frequency of differences between x and y.

Finite Hamming distance:

$$d_{13\times 8}(x, y) = \frac{}{13\times 8}$$

Besicovitch Distance

$x|y$

×	○	×	○	×	○	×	○	×	○	×	○	×
○	⊠	⊠	⊠	○	×	⊠	⊠	⊠	⊠	⊠	⊠	⊠
×	○	⊠	○	⊠	○	×	⊠	⊠	○	×	○	×
○	×	⊠	×	○	×	○	×	○	×	○	×	○
×	○	×	⊠	×	⊠	⊠	○	⊠	○	⊠	○	×
○	⊠	⊠	×	⊠	×	○	×	○	⊠	⊠	⊠	⊠
×	⊠	×	○	×	○	⊠	⊠	×	○	⊠	○	×
○	×	○	×	○	×	⊠	×	⊠	×	○	×	○

Figure 7: Frequency of differences between x and y.

Finite Hamming distance:

$$d_{13\times 8}(x,y) = \frac{33}{13\times 8} \approx 0.3$$

Besicovitch Distance

$x|y$

×	○	×	○	×	○	×	○	×	○	×	○	×
○	⊠	⊠	⊠	○	×	⊠	⊠	⊠	⊠	⊠	⊠	⊠
×	○	⊠	○	⊠	○	×	⊠	⊠	○	×	○	×
○	×	⊠	×	○	×	○	×	○	×	○	×	○
×	○	×	⊠	×	⊠	⊠	○	⊠	○	⊠	○	×
○	⊠	⊠	×	⊠	×	○	×	○	⊠	⊠	⊠	⊠
×	⊠	×	○	×	○	⊠	⊠	×	○	⊠	○	×
○	×	○	×	○	×	⊠	×	⊠	×	○	×	○

Figure 7: Frequency of differences between x and y.

Finite Hamming distance:

$$d_{13\times 8}(x,y) = \frac{33}{13\times 8} \approx 0.3$$

Hamming-Besicovitch pseudo-distance:

$$d_H = \limsup_{n\to\infty} d_{n\times n}$$

Besicovitch Distance

$x|y$

×	○	×	○	×	○	×	○	×	○	×	○	×
○	⊠	⊠	⊠	○	×	⊠	⊠	⊠	⊠	⊠	⊠	⊠
×	○	⊠	○	⊠	○	×	⊠	⊠	○	×	○	×
○	×	⊠	×	○	×	○	×	○	×	○	×	○
×	○	×	⊠	×	⊠	⊠	○	⊠	○	⊠	○	×
○	⊠	⊠	×	⊠	×	○	×	○	⊠	⊠	⊠	⊠
×	⊠	×	○	×	○	⊠	⊠	×	○	⊠	○	×
○	×	○	×	○	×	⊠	×	⊠	×	○	×	○

Figure 7: Frequency of differences between x and y.

Finite Hamming distance:

$$d_{13\times 8}(x,y) = \frac{33}{13\times 8} \approx 0.3$$

Hamming-Besicovitch pseudo-distance:

$$d_H = \limsup_{n\to\infty} d_{n\times n}$$

Besicovitch distance on σ-invariant measures:

$$d_B(\mu,\nu) := \inf_{\lambda \text{ a coupling}} \int d_H(x,y)\mathrm{d}\lambda(x,y) = \inf_{\lambda \text{ a coupling}} \lambda\left([x_0 \neq y_0]\right)$$

Stability

Definition (Speed of Stability)

Let f s.t. $\lim_{x \to 0^+} f(x) = 0$. The SFT $\Omega_{\mathcal{F}}$ is f-stable for d_B on Bernoulli noises if:

$$\forall \varepsilon > 0, \quad \sup_{\lambda \in \widetilde{\mathcal{M}}^{\mathcal{B}}_{\mathcal{F}}(\varepsilon)} d_B\left(\pi_1^*(\lambda), \mathcal{M}_{\mathcal{F}}\right) \leq f(\varepsilon).$$

Informally, a generic ε-noisy configuration will be at distance $f(\varepsilon)$ of a tiling in $\Omega_{\mathcal{F}}$.

Stability

Definition (Speed of Stability)

Let f s.t. $\lim_{x \to 0^+} f(x) = 0$. The SFT $\Omega_{\mathcal{F}}$ is f-stable for d_B on Bernoulli noises if:

$$\forall \varepsilon > 0, \quad \sup_{\lambda \in \widetilde{\mathcal{M}}^{\mathcal{B}}_{\mathcal{F}}(\varepsilon)} d_B\left(\pi_1^*(\lambda), \mathcal{M}_{\mathcal{F}}\right) \leq f(\varepsilon).$$

Informally, a generic ε-noisy configuration will be at distance $f(\varepsilon)$ of a tiling in $\Omega_{\mathcal{F}}$.

For the Diluted Domino tileset:

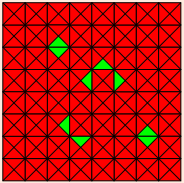

Figure 8:

Stability

Definition (Speed of Stability)

Let f s.t. $\lim_{x \to 0^+} f(x) = 0$. The SFT $\Omega_{\mathcal{F}}$ is f-stable for d_B on Bernoulli noises if:

$$\forall \varepsilon > 0, \quad \sup_{\lambda \in \widetilde{\mathcal{M}}^{\mathcal{B}}_{\mathcal{F}}(\varepsilon)} d_B\left(\pi_1^*(\lambda), \mathcal{M}_{\mathcal{F}}\right) \leq f(\varepsilon).$$

Informally, a generic ε-noisy configuration will be at distance $f(\varepsilon)$ of a tiling in $\Omega_{\mathcal{F}}$.

For the Diluted Domino tileset:

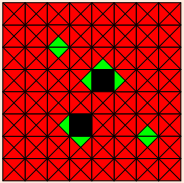

Figure 8: Around obscured cells,

Stability

Definition (Speed of Stability)

Let f s.t. $\lim_{x \to 0^+} f(x) = 0$. The SFT $\Omega_{\mathcal{F}}$ is f-stable for d_B on Bernoulli noises if:

$$\forall \varepsilon > 0, \quad \sup_{\lambda \in \widetilde{\mathcal{M}}^{\mathcal{B}}_{\mathcal{F}}(\varepsilon)} d_B\left(\pi_1^*(\lambda), \mathcal{M}_{\mathcal{F}}\right) \leq f(\varepsilon).$$

Informally, a generic ε-noisy configuration will be at distance $f(\varepsilon)$ of a tiling in $\Omega_{\mathcal{F}}$.

For the Diluted Domino tileset:

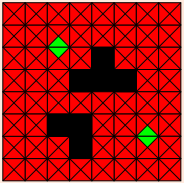

Figure 8: Around obscured cells, we clear the neighbourhood,

Stability

Definition (Speed of Stability)

Let f s.t. $\lim_{x \to 0^+} f(x) = 0$. The SFT $\Omega_{\mathcal{F}}$ is f-stable for d_B on Bernoulli noises if:

$$\forall \varepsilon > 0, \quad \sup_{\lambda \in \widetilde{\mathcal{M}}^{\mathcal{B}}_{\mathcal{F}}(\varepsilon)} d_B\left(\pi_1^*(\lambda), \mathcal{M}_{\mathcal{F}}\right) \leq f(\varepsilon).$$

Informally, a generic ε-noisy configuration will be at distance $f(\varepsilon)$ of a tiling in $\Omega_{\mathcal{F}}$.

For the Diluted Domino tileset:

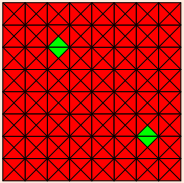

Figure 8: Around obscured cells, we clear the neighbourhood, and obtain a valid tiling.

Stability

Definition (Speed of Stability)

Let f s.t. $\lim_{x \to 0^+} f(x) = 0$. The SFT $\Omega_{\mathcal{F}}$ is f-stable for d_B on Bernoulli noises if:

$$\forall \varepsilon > 0, \quad \sup_{\lambda \in \widetilde{\mathcal{M}}^{\mathcal{B}}_{\mathcal{F}}(\varepsilon)} d_B\left(\pi_1^*(\lambda), \mathcal{M}_{\mathcal{F}}\right) \leq f(\varepsilon).$$

Informally, a generic ε-noisy configuration will be at distance $f(\varepsilon)$ of a tiling in $\Omega_{\mathcal{F}}$.

For the Diluted Domino tileset:

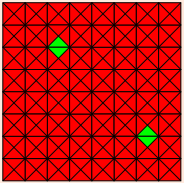

Figure 8: Around obscured cells, we clear the neighbourhood, and obtain a valid tiling.

Hence, this example is 5ε-stable.

Conjugacy Invariance

Theorem [Gayral and Sablik, 2021, Corollary 3.15]

Let $f : \Omega_{\mathcal{F}} \to \Omega_{\mathcal{F}'}$ be a conjugacy, a bi-continuous bijection, such that, for any $k \in \mathbb{Z}^d$, we have $\sigma_k \circ f = f \circ \sigma_k$.

Then $\Omega_{\mathcal{F}}$ is stable iff $\Omega_{\mathcal{F}'}$ is. In other words, stability is a conjugacy invariant.

Conjugacy Invariance

Theorem [Gayral and Sablik, 2021, Corollary 3.15]

Let $f : \Omega_{\mathcal{F}} \to \Omega_{\mathcal{F}'}$ be a conjugacy, a bi-continuous bijection, such that, for any $k \in \mathbb{Z}^d$, we have $\sigma_k \circ f = f \circ \sigma_k$.

Then $\Omega_{\mathcal{F}}$ is stable iff $\Omega_{\mathcal{F}'}$ is. In other words, stability is a conjugacy invariant.

What kind of (in)stability results can we expect from typical SFTs?

Conjugacy Invariance

Theorem [Gayral and Sablik, 2021, Corollary 3.15]

Let $f : \Omega_{\mathcal{F}} \to \Omega_{\mathcal{F}'}$ be a conjugacy, a bi-continuous bijection, such that, for any $k \in \mathbb{Z}^d$, we have $\sigma_k \circ f = f \circ \sigma_k$.

Then $\Omega_{\mathcal{F}}$ is stable iff $\Omega_{\mathcal{F}'}$ is. In other words, stability is a conjugacy invariant.

What kind of (in)stability results can we expect from typical SFTs?

A fixed-point argument [Durand et al., 2012] already gave a stable aperiodic example.

Stability for Periodic Tilings

1D Classification of the Stability

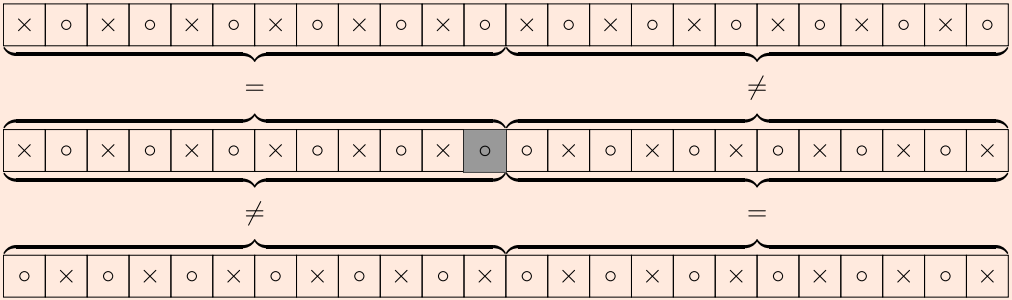

Figure 9: The noisy configuration is at Hamming distance $\frac{1}{2}$ of the clear $(\times\circ\times\circ)^{\infty}$ ones.

1D Classification of the Stability

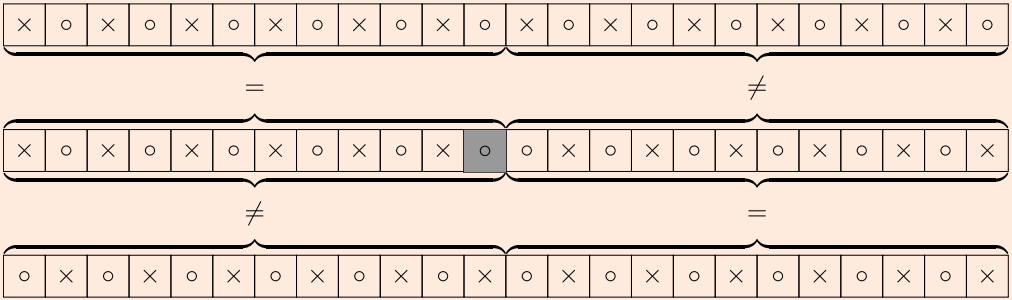

Figure 9: The noisy configuration is at Hamming distance $\frac{1}{2}$ of the clear $(\times\circ\times\circ)^\infty$ ones.

Theorem [Gayral and Sablik, 2021, Theorem 4.8 and Theorem 4.9]

Consider $\Omega_{\mathcal{F}}$ a 1D SFT. Then $\Omega_{\mathcal{F}}$ is (linearly) stable on Bernoulli noises iff it is mixing.

Most notably, p-periodic SFTs (with $p \geq 2$) are unstable.

Periodic Tilings in Higher Dimensions

A SFT $\Omega_{\mathcal{F}}$ is (strongly) periodic if there exists an integer N such that any configuration is invariant for any translation in $(N\mathbb{Z})^d$.

Theorem [Gayral and Sablik, 2021, Theorem 5.7]

Consider $\Omega_{\mathcal{F}}$ a 2D+ periodic SFT.

Then $\Omega_{\mathcal{F}}$ is f-stable on Bernoulli noises, with linear speed $f(\varepsilon) = 2C^d_{c(\mathcal{F})}\varepsilon$.

Reconstruction Function

Lemma [Gayral and Sablik, 2021, Lemma 5.3]

Consider a 2D+ periodic SFT $\Omega_{\mathcal{F}}$.

There exists $c(\mathcal{F}) \geq \lceil \frac{N}{2} \rceil$ such that, for any connected cell window $I \subset \mathbb{Z}^d$, if $w \in \mathcal{A}^{I+B_c}$ is locally admissible, then $w|_I$ is globally admissible.

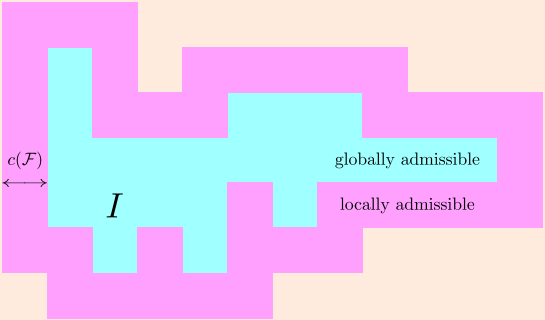

Figure 10: Here, the whole domain contains no forbidden pattern, but only the blue zone is guaranteed to be the restriction of an actual configuration.

Thickened Percolation

Consider $\varphi_n(b)_x = \max_{\|y-x\|_\infty \leq n} b_y$ for $b \in \{0,1\}^{\mathbb{Z}^d}$.

Starting from a site percolation ν, we obtain the n-thickened percolation $\varphi_n^*(\nu)$.

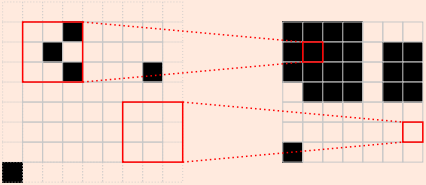

Figure 11: Illustration of the mapping φ_1.

Proposition [Gayral and Sablik, 2021, Proposition 5.6]

Consider $I \subset \mathbb{Z}^d$ the random infinite component of the n-thickened $\mathcal{B}(\varepsilon)^{\otimes \mathbb{Z}^d}$-percolation.

Then $C_n^d = 48(2n+1)^d$ is such that $\mathbb{P}(0 \notin I) \leq C_n^d \times \varepsilon$.

Stability for Aperiodic Tilings

The Robinson Tiling

The (Enhanced) Robinson Tiling

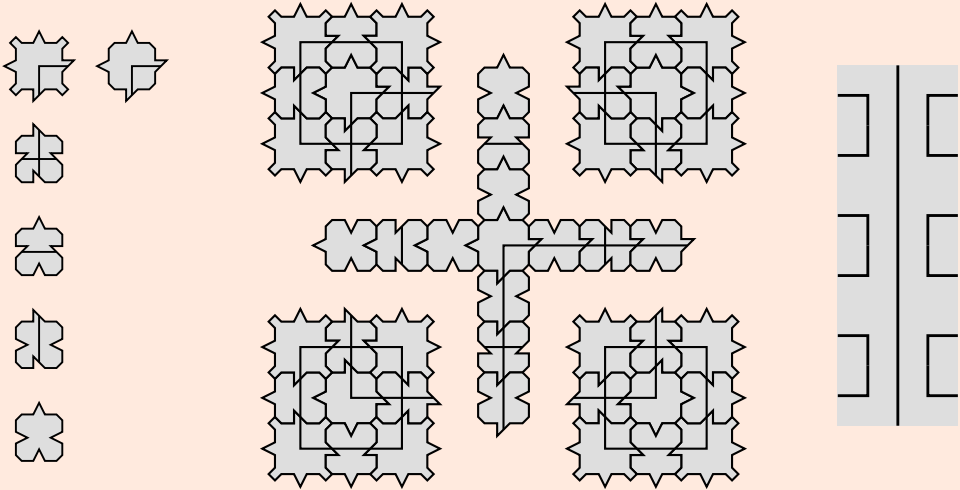

Figure 12: Tileset and hierarchical structure of the Robinson tiling,

The (Enhanced) Robinson Tiling

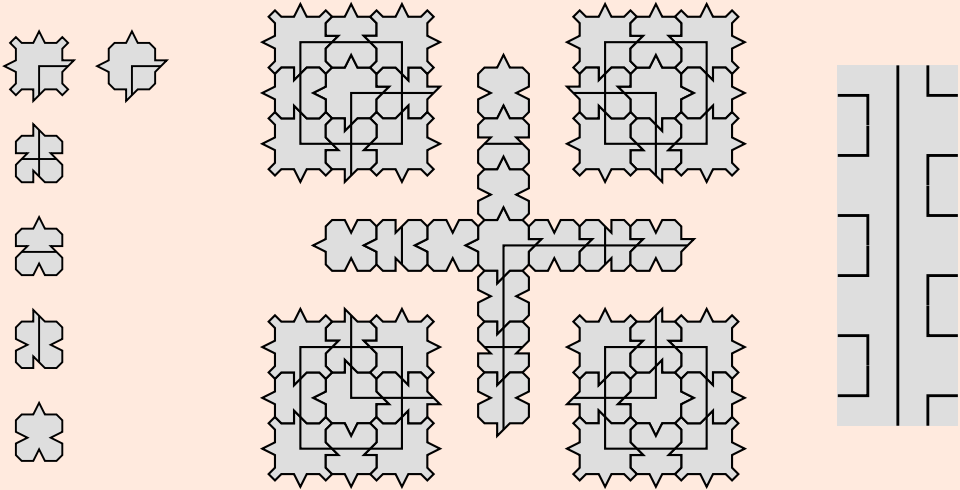

Figure 12: Tileset and hierarchical structure of the Robinson tiling,

The (Enhanced) Robinson Tiling

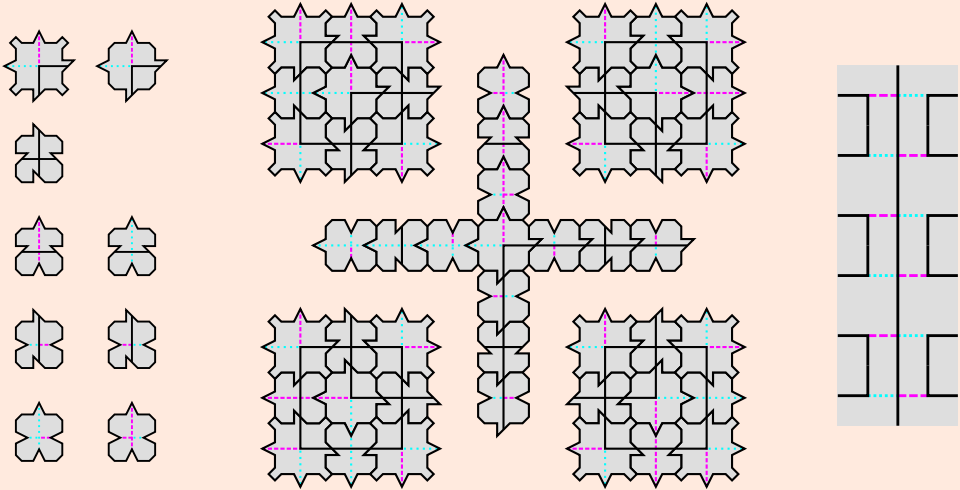

Figure 12: Tileset and hierarchical structure of the Robinson tiling, with strengthened local rules.

High-Density Quasi-Periodic Structure

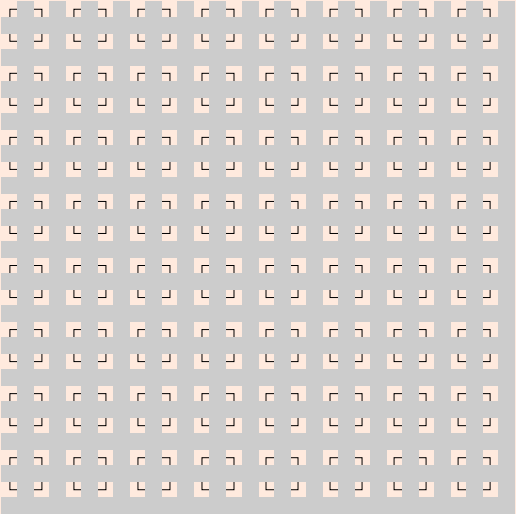

Figure 13: The density of the grid around N-macro-tiles goes to 0 as $N \to \infty$.

High-Density Quasi-Periodic Structure

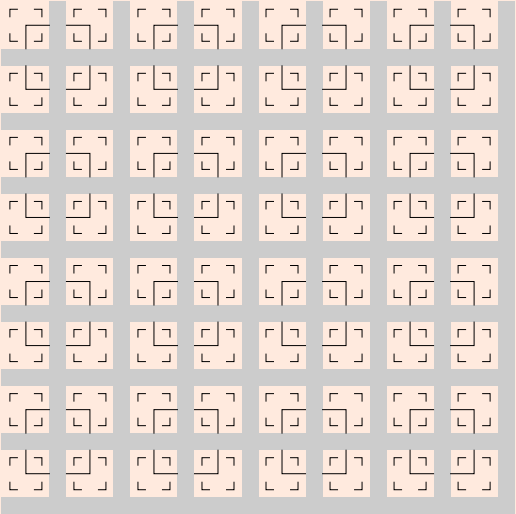

Figure 13: The density of the grid around N-macro-tiles goes to 0 as $N \to \infty$.

High-Density Quasi-Periodic Structure

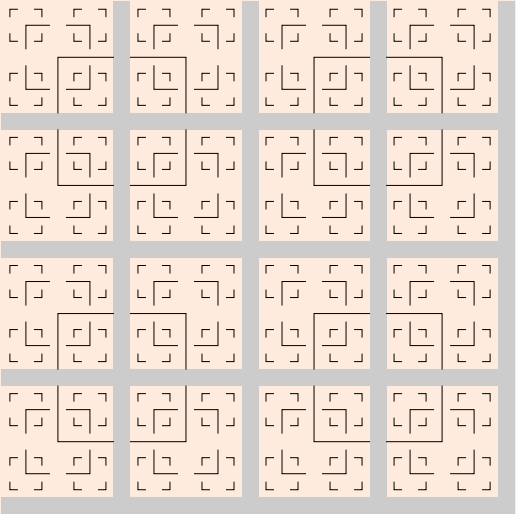

Figure 13: The density of the grid around N-macro-tiles goes to 0 as $N \to \infty$.

Stability for Aperiodic Tilings

Aperiodic Stability

Reconstruction Function for the Enhanced Tiling

Proposition [Gayral and Sablik, 2021, Proposition 7.7]

For any scale $N \geq 2$, the constant $C_N = 2^N - 1$ is such that
for any integer n and any clear locally admissible pattern w on B_{n+C_N},
$w|_{B_n}$ is almost globally admissible, in the sense that up to a low-density grid,
$w|_{B_n}$ is made of well-aligned and well-oriented N-macro-tiles.

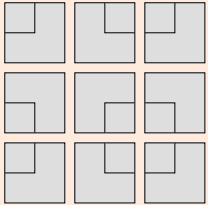

Figure 14: Family of well-aligned and well-oriented tiles.

Non-linear Polynomial Stability

Theorem [Gayral and Sablik, 2021, Proposition 7.8 and Theorem 7.9]

For any $\varepsilon > 0$, any scale N, and any measure $\mu = \pi_1^*(\lambda)$ with $\lambda \in \widetilde{\mathcal{M}_{\mathcal{F}}^{\mathcal{B}}}(\varepsilon)$:

$$d_B(\mu, \mathcal{M}_{\mathcal{F}}) \leq 96\left(2^{N+2}+1\right)^2 \varepsilon + \frac{1}{2^{N-1}}.$$

Hence, the SFT is f-stable with $f(\varepsilon) = 48\sqrt[3]{6\varepsilon}$.

Could we obtain faster bounds for an aperiodic tiling?

Stability for Aperiodic Tilings

Aperiodic Unstability

A Two-Coloured Robinson Tiling

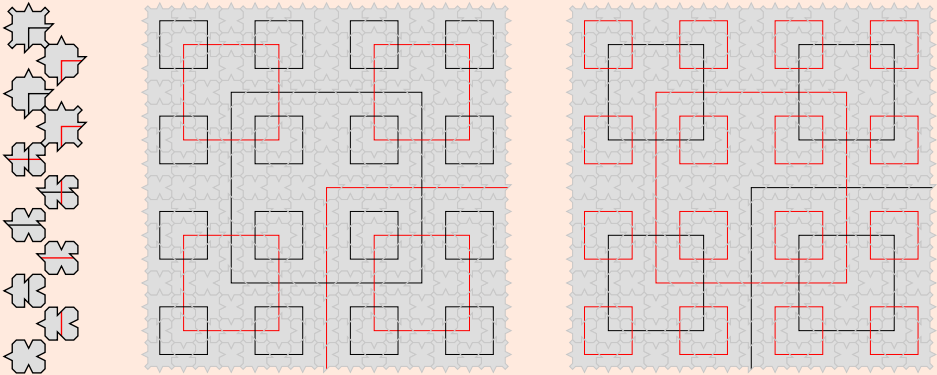

Figure 15: Two-coloured Robinson structure.

Unstable Colour Flips

Proposition [Gayral, 2021, Proposition 1]

The SFT Ω_{RB} is unstable.

More precisely, for any $\varepsilon > 0$, we have $\mu \in \mathcal{M}_{RB}^{\mathcal{B}}(\varepsilon)$ such that $d_B(\mu, \mathcal{M}_{RB}) \geq \frac{1}{8}$.

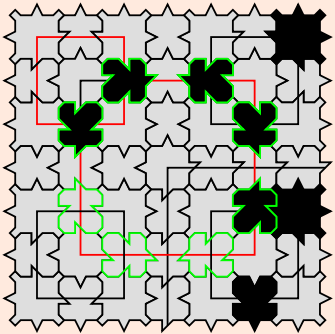

Figure 16: The Red-Black alternating structure allows for colour flips.

Closing Thoughts

Stability for the Domino Tiling?

- For the Diluted Domino tileset:

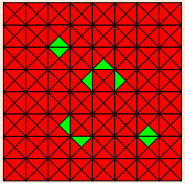

Figure 17:

Stability for the Domino Tiling?

- For the Diluted Domino tileset:

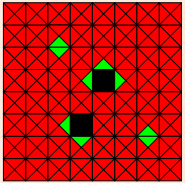

Figure 17: Around obscured cells,

Stability for the Domino Tiling?

- For the Diluted Domino tileset:

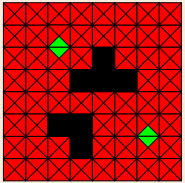

Figure 17: Around obscured cells, we clear the neighbourhood,

Stability for the Domino Tiling?

- For the Diluted Domino tileset:

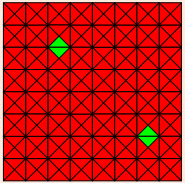

Figure 17: Around obscured cells, we clear the neighbourhood, and obtain a valid tiling.

Stability for the Domino Tiling?

- For the Diluted Domino tileset:

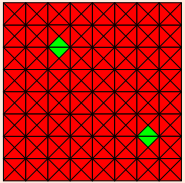

Figure 17: Around obscured cells, we clear the neighbourhood, and obtain a valid tiling.

- What about the Dense Domino phase, without the  tile?

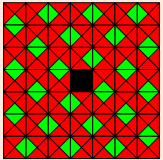

Figure 18: To pair the obscured tile as a domino, we must break another domino.

Other Open Questions

- Can we have Besicovitch-stability for Gibbs measures as the temperature goes to 0?
- Can we link stability with dynamical properties of the SFTs?
  (*e.g.* block gluing, unique ergodicity, etc.)
- Can we generalise some results to other groups G with well-behaved percolations?

Bibliography

Léo Gayral and Mathieu Sablik.
On the Besicovitch-stability of noisy random tilings.
arxiv.org/abs/2104.09885v2, 2021.

Bruno Durand, Andrei Romashchenko, and Alexander Shen.
Fixed-point tile sets and their applications.
Journal of Computer and System Sciences, 78(3):731–764, 2012.

Léo Gayral.
The Besicovitch-stability of noisy tilings is undecidable.
hal.archives-ouvertes.fr/hal-03233596, 2021.

THE END OF PRESENTATION

ONE MORE SLIDE:

Thank you.

Appendices

Undecidability of the Stability

Σ_1-Hardness of the Problem

Turing Machine Space-Time Diagrams as Tilings

Consider a Turing machine $(Q, \Gamma, I, F, \delta)$ and define the following Wang tiles:

- For any letter $a \in \Gamma$ and any state $q \in Q$:

- For any letter $a \in \Gamma$ and initial state $q \in I$:

- For any letter $a \in \Gamma$ and final state $q \in F$:

- For any transition $\delta(a, q) = (b, q', L)$:

- For any transition $\delta(a, q) = (b, q', R)$:

Embedding Space-Time Diagrams into Robinson Tilings

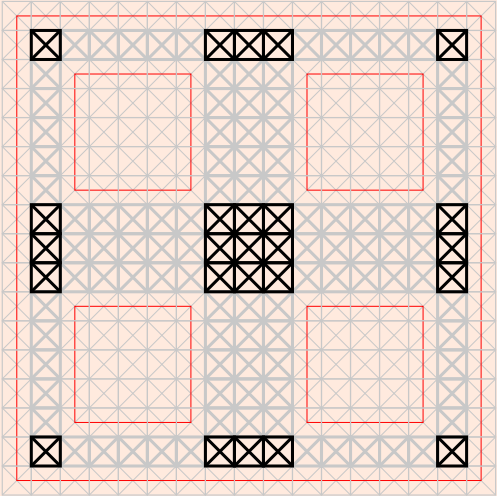

Figure 19: The free black tiles encode the diagram, the grey ones are communication channels.

A Four-Coloured Enhanced Robinson Tiling

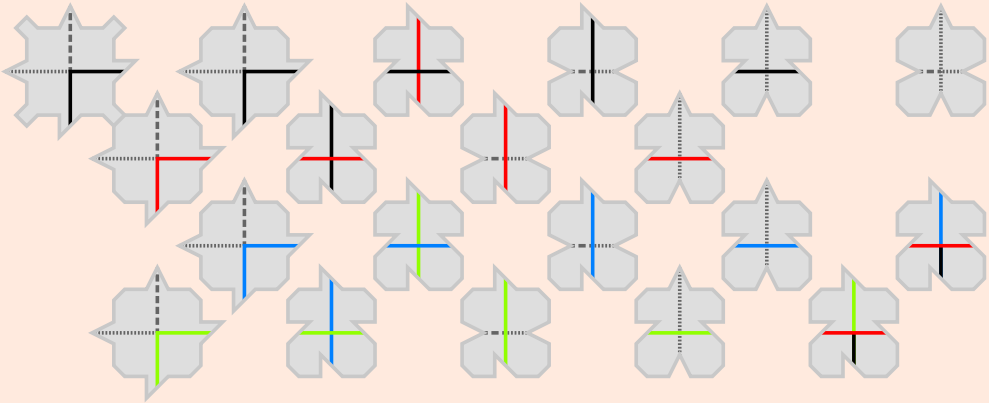

Figure 20: The tiling uses an enhanced Robinson structure.
It starts with Black bumpy tiles, alternates between Red and Black,
then may transition to an unstable Blue-Green regime.

Transition from the Red-Black to the Blue-Green Phase

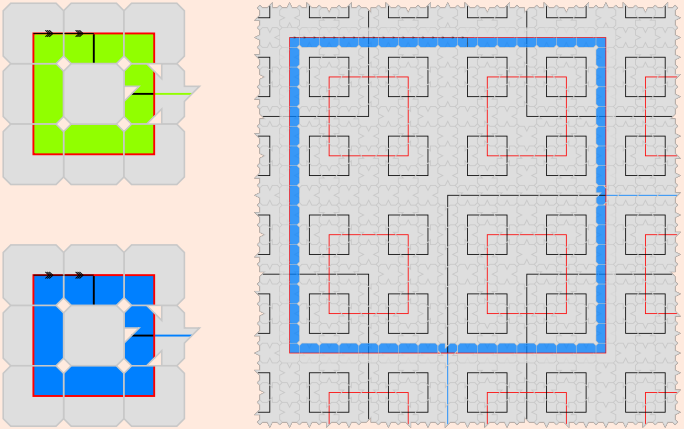

Figure 21: The flow layer appears *iff* there is a final state, and propagates the colour on the border.

Undecidability of the Stability

Theorem [Gayral, 2021, Theorem 1]

Denote $\mathcal{F}_T$ the SFT that embeds the Turing machine T into a Robinson tiling.

Then $\mathcal{F}_T$ is stable (for d_B on the class $\mathcal{B}$) iff T does not halt on the empty input.

In the stable case, $\mathcal{F}_T$ is polynomially stable.

Because the halting problem is Σ_1-hard, so is the question of unstability.

Theorem

Stability is Π_1-hard.

Idea for the Stable Case: All N-Macro-Tiles Are Mostly the Same

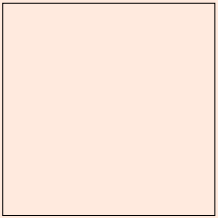

Figure 22: In a $2N$-macro-tile, only $O\left(12^N\right)$ tiles out of 16^N are ignored.

This gives a $16^N \times C\varepsilon + \left(\frac{3}{4}\right)^N$ bound on d_B at scale $2N$.

Idea for the Stable Case: All N-Macro-Tiles Are Mostly the Same

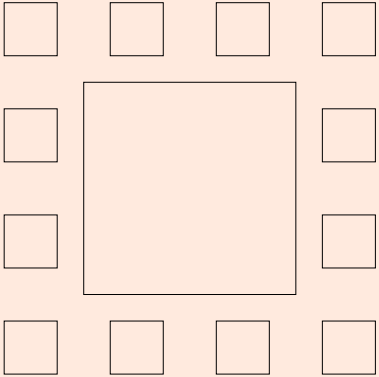

Figure 22: In a $2N$-macro-tile, only $O\left(12^N\right)$ tiles out of 16^N are ignored.

This gives a $16^N \times C\varepsilon + \left(\frac{3}{4}\right)^N$ bound on d_B at scale $2N$.

Idea for the Stable Case: All N-Macro-Tiles Are Mostly the Same

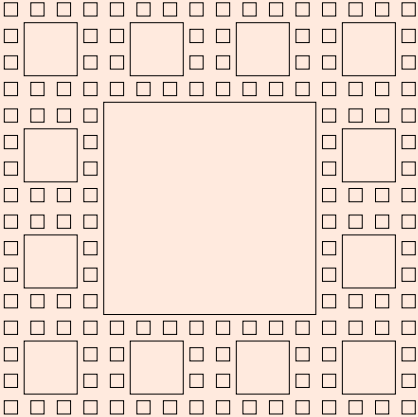

Figure 22: In a $2N$-macro-tile, only $O\left(12^N\right)$ tiles out of 16^N are ignored.

This gives a $16^N \times C\varepsilon + \left(\frac{3}{4}\right)^N$ bound on d_B at scale $2N$.

Idea for the Stable Case: All N-Macro-Tiles Are Mostly the Same

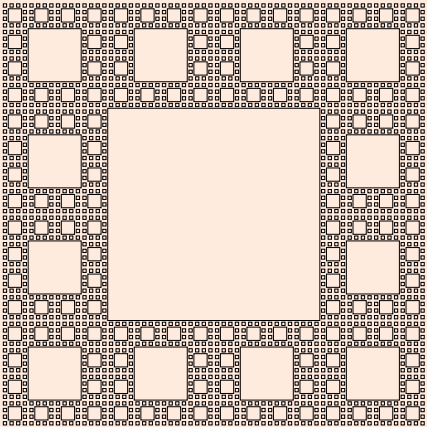

Figure 22: In a $2N$-macro-tile, only $O\left(12^N\right)$ tiles out of 16^N are ignored.

This gives a $16^N \times C\varepsilon + \left(\frac{3}{4}\right)^N$ bound on d_B at scale $2N$.

Idea for the Unstable Case: Two Kinds of Widely Different N-Macro-Tiles

We can do the same Blue-Green colour flip as in our Red-Black unstable example.

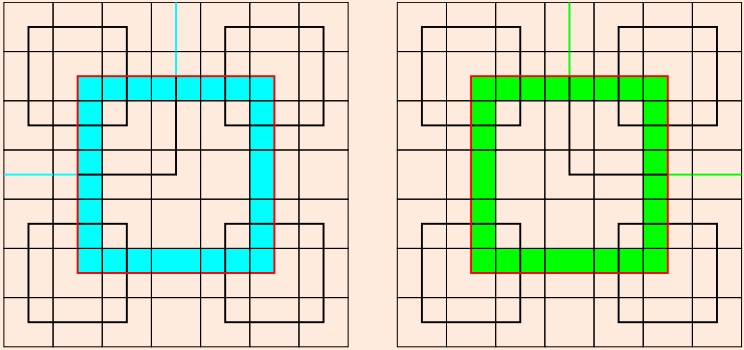

Figure 23: The transition scale plays the role of 1-macro-tiles for the Blue-Green phase.

If the Turing machine stops in the $2N$-macro-tiles,
we guarantee a $\Omega\left(\frac{1}{16^N}\right)$ density of differences between Blue and Green.

Dual Construction for Σ_1-Hard Stability

We now use the following Robinson structure:

- Encode two bits (a, b) in the central arm.
- The Red-Black bit a starts as Black and then alternates, for the Turing structure.
- The Blue-Green bit b starts freely and then alternates.
- Whenever the machine stops (necessarily a is Black), b *must* be Blue.

Dual Construction for Σ_1-Hard Stability

We now use the following Robinson structure:

- Encode two bits (a, b) in the central arm.
- The Red-Black bit a starts as Black and then alternates, for the Turing structure.
- The Blue-Green bit b starts freely and then alternates.
- Whenever the machine stops (necessarily a is Black), b *must* be Blue.

Dual Construction for Σ_1-Hard Stability

We now use the following Robinson structure:

- Encode two bits (a, b) in the central arm.
- The Red-Black bit a starts as Black and then alternates, for the Turing structure.
- The Blue-Green bit b starts freely and then alternates.
- Whenever the machine stops (necessarily a is Black), b *must* be Blue.

Dual Construction for Σ_1-Hard Stability

We now use the following Robinson structure:

- Encode two bits (a, b) in the central arm.
- The Red-Black bit a starts as Black and then alternates, for the Turing structure.
- The Blue-Green bit b starts freely and then alternates.
- Whenever the machine stops (necessarily a is Black), b *must* be Blue.

Dual Construction for Σ_1-Hard Stability

We now use the following Robinson structure:

- Encode two bits (a, b) in the central arm.
- The Red-Black bit a starts as Black and then alternates, for the Turing structure.
- The Blue-Green bit b starts freely and then alternates.
- Whenever the machine stops (necessarily a is Black), b *must* be Blue.

Thence:

T halts	$\Rightarrow$	One kind of macro-tiles only at big-enough scales	$\Rightarrow$	Stable
T doesn't stop	$\Rightarrow$	Two kinds of different macro-tiles at all the scales	$\Rightarrow$	Unstable

Dual Construction for Σ_1-Hard Stability

We now use the following Robinson structure:

- Encode two bits (a, b) in the central arm.
- The Red-Black bit a starts as Black and then alternates, for the Turing structure.
- The Blue-Green bit b starts freely and then alternates.
- Whenever the machine stops (necessarily a is Black), b *must* be Blue.

Thence:

T halts	$\Rightarrow$	One kind of macro-tiles only at big-enough scales	$\Rightarrow$	Stable
T doesn't stop	$\Rightarrow$	Two kinds of different macro-tiles at all the scales	$\Rightarrow$	Unstable

Dual Construction for Σ_1-Hard Stability

We now use the following Robinson structure:

- Encode two bits (a, b) in the central arm.
- The Red-Black bit a starts as Black and then alternates, for the Turing structure.
- The Blue-Green bit b starts freely and then alternates.
- Whenever the machine stops (necessarily a is Black), b *must* be Blue.

Thence:

T halts	$\Rightarrow$	One kind of macro-tiles only at big-enough scales	$\Rightarrow$	Stable
T doesn't stop	$\Rightarrow$	Two kinds of different macro-tiles at all the scales	$\Rightarrow$	Unstable

Dual Construction for Σ_1-Hard Stability

We now use the following Robinson structure:

- Encode two bits (a, b) in the central arm.
- The Red-Black bit a starts as Black and then alternates, for the Turing structure.
- The Blue-Green bit b starts freely and then alternates.
- Whenever the machine stops (necessarily a is Black), b *must* be Blue.

Thence:

T halts	$\Rightarrow$	One kind of macro-tiles only at big-enough scales	$\Rightarrow$	Stable
T doesn't stop	$\Rightarrow$	Two kinds of different macro-tiles at all the scales	$\Rightarrow$	Unstable

Theorem

Stability is Σ_1-hard.

Undecidability of the Stability

Climbing the Arithmetical Hierarchy

Toeplitz Encoding of a Sequence

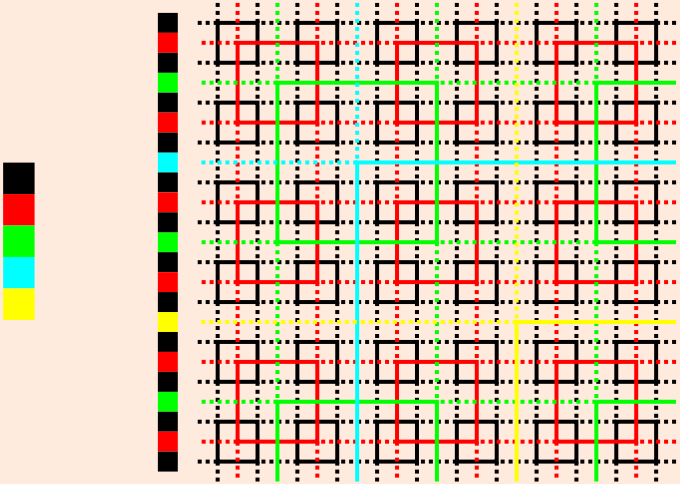

Figure 24: Toeplitz encoding of the sequence of colours on the left into the Robinson hierarchy.

Toeplitz Encoding of a Sequence

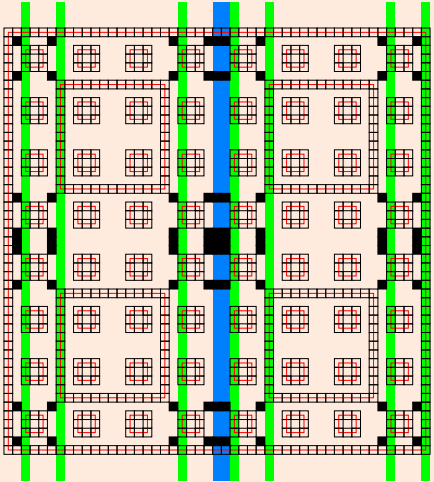

Figure 25: In practice, we see a finite prefix of the Toeplitz encoding as a read-only input.

Generalising the Σ_1-Hard Construction on Toeplitz Inputs

Consider a Turing machine T with the alphabet $\Gamma = \Sigma \sqcup \{\#\}$.

We encode a word $w \in \Sigma^*\{\#\}^*$ of length N in a $(2N+1)$-macro-tile.

We have three phases in the Robinson hierarchy:

1. Decoding of the Toeplitz sequence into a word $w \in \Sigma^*$.

$\Downarrow$

Ignition of the unstable Blue-Green bit.

$\Downarrow$

2. Partial computation of T on the input w.

$\Downarrow$

Freezing of the now stable Blue-Green bit.

$\Downarrow$

3. T halts on w.

Generalising the Σ_1-Hard Construction on Toeplitz Inputs

Consider a Turing machine T with the alphabet $\Gamma = \Sigma \sqcup \{\#\}$.

We encode a word $w \in \Sigma^*\{\#\}^*$ of length N in a $(2N+1)$-macro-tile.

We have three phases in the Robinson hierarchy:

1. Decoding of the Toeplitz sequence into a word $w \in \Sigma^*$.

$\Downarrow$

Ignition of the unstable Blue-Green bit.

$\Downarrow$

2. Partial computation of T on the input w.

$\Downarrow$

Freezing of the now stable Blue-Green bit.

$\Downarrow$

3. T halts on w.

Generalising the Σ_1-Hard Construction on Toeplitz Inputs

Consider a Turing machine T with the alphabet $\Gamma = \Sigma \sqcup \{\#\}$.

We encode a word $w \in \Sigma^*\{\#\}^*$ of length N in a $(2N+1)$-macro-tile.

We have three phases in the Robinson hierarchy:

1. Decoding of the Toeplitz sequence into a word $w \in \Sigma^*$.

$\Downarrow$

Ignition of the unstable Blue-Green bit.

$\Downarrow$

2. Partial computation of T on the input w.

$\Downarrow$

Freezing of the now stable Blue-Green bit.

$\Downarrow$

3. T halts on w.

Generalising the Σ_1-Hard Construction on Toeplitz Inputs

Consider a Turing machine T with the alphabet $\Gamma = \Sigma \sqcup \{\#\}$.

We encode a word $w \in \Sigma^*\{\#\}^*$ of length N in a $(2N+1)$-macro-tile.

We have three phases in the Robinson hierarchy:

1. Decoding of the Toeplitz sequence into a word $w \in \Sigma^*$.

$\Downarrow$

Ignition of the unstable Blue-Green bit.

$\Downarrow$

2. Partial computation of T on the input w.

$\Downarrow$

Freezing of the now stable Blue-Green bit.

$\Downarrow$

3. T halts on w.

Generalising the Σ_1-Hard Construction on Toeplitz Inputs

Consider a Turing machine T with the alphabet $\Gamma = \Sigma \sqcup \{\#\}$.

We encode a word $w \in \Sigma^*\{\#\}^*$ of length N in a $(2N+1)$-macro-tile.

We have three phases in the Robinson hierarchy:

1. Decoding of the Toeplitz sequence into a word $w \in \Sigma^*$.

$\Downarrow$

Ignition of the unstable Blue-Green bit.

$\Downarrow$

2. Partial computation of T on the input w.

$\Downarrow$

Freezing of the now stable Blue-Green bit.

$\Downarrow$

3. T halts on w.

Generalising the Σ_1-Hard Construction on Toeplitz Inputs

Consider a Turing machine T with the alphabet $\Gamma = \Sigma \sqcup \{\#\}$.

We encode a word $w \in \Sigma^*\{\#\}^*$ of length N in a $(2N+1)$-macro-tile.

We have three phases in the Robinson hierarchy:

1. Decoding of the Toeplitz sequence into a word $w \in \Sigma^*$.

$$\Downarrow$$

Ignition of the unstable Blue-Green bit.

$$\Downarrow$$

2. Partial computation of T on the input w.

$$\Downarrow$$

Freezing of the now stable Blue-Green bit.

$$\Downarrow$$

3. T halts on w.

Stability is Π_2-Hard

We have 3 situations globally speaking:

- Infinite decoding of an input $w \in \Sigma^{\mathbb{N}}$: stable.
- Halting of T on $w \in \Sigma^*$: stable.
- Infinite computation of T on $w \in \Sigma^*$: unstable through colour flips.

We have a family of bounds of the form:

$$d_B\left(\mu_\varepsilon, \mathcal{M}_{\mathcal{F}_T}\right) \leq 16^{\varphi(N)} \times C\varepsilon + \left(\frac{3}{4}\right)^N,$$

with $\varphi(N)$ the scale at which T has halted on all the inputs of length at most N.

If T halts on all the inputs, the bound still goes to 0 as $\varepsilon \to 0$,
but cannot be explicit as φ can be bigger than any computable function.

Theorem

$\mathcal{F}_T$ is stable iff T stops on all its entries, which is a Π_2-complete problem.

Stability is Π_2-Hard

We have 3 situations globally speaking:

- Infinite decoding of an input $w \in \Sigma^{\mathbb{N}}$: stable.
- Halting of T on $w \in \Sigma^*$: stable.
- Infinite computation of T on $w \in \Sigma^*$: unstable through colour flips.

We have a family of bounds of the form:

$$d_B\left(\mu_\varepsilon, \mathcal{M}_{\mathcal{F}_T}\right) \leq 16^{\varphi(N)} \times C\varepsilon + \left(\frac{3}{4}\right)^N,$$

with $\varphi(N)$ the scale at which T has halted on all the inputs of length at most N.

If T halts on all the inputs, the bound still goes to 0 as $\varepsilon \to 0$,
but cannot be explicit as φ can be bigger than any computable function.

Theorem

$\mathcal{F}_T$ is stable iff T stops on all its entries, which is a Π_2-complete problem.

Stability is Π_2-Hard

We have 3 situations globally speaking:

- Infinite decoding of an input $w \in \Sigma^{\mathbb{N}}$: stable.
- Halting of T on $w \in \Sigma^*$: stable.
- Infinite computation of T on $w \in \Sigma^*$: unstable through colour flips.

We have a family of bounds of the form:

$$d_B\left(\mu_\varepsilon, \mathcal{M}_{\mathcal{F}_T}\right) \leq 16^{\varphi(N)} \times C\varepsilon + \left(\frac{3}{4}\right)^N,$$

with $\varphi(N)$ the scale at which T has halted on all the inputs of length at most N.

If T halts on all the inputs, the bound still goes to 0 as $\varepsilon \to 0$,
but cannot be explicit as φ can be bigger than any computable function.

Theorem

$\mathcal{F}_T$ is stable iff T stops on all its entries, which is a Π_2-complete problem.

Stability is Π_2-Hard

We have 3 situations globally speaking:

- Infinite decoding of an input $w \in \Sigma^{\mathbb{N}}$: stable.
- Halting of T on $w \in \Sigma^*$: stable.
- Infinite computation of T on $w \in \Sigma^*$: unstable through colour flips.

We have a family of bounds of the form:

$$d_B\left(\mu_\varepsilon, \mathcal{M}_{\mathcal{F}_T}\right) \leq 16^{\varphi(N)} \times C\varepsilon + \left(\frac{3}{4}\right)^N,$$

with $\varphi(N)$ the scale at which T has halted on all the inputs of length at most N.

If T halts on all the inputs, the bound still goes to 0 as $\varepsilon \to 0$,
but cannot be explicit as φ can be bigger than any computable function.

Theorem

$\mathcal{F}_T$ is stable iff T stops on all its entries, which is a Π_2-complete problem.

Undecidability of the Stability

Finding an Upper Bound

Could the Problem be Π_2-Complete?

Stability of $\Omega_{\mathcal{F}}$: $\forall \delta > 0, \exists \varepsilon > 0, \quad \sup_{\mu \in \mathcal{M}_{\mathcal{F}}^{\mathbb{R}}(\varepsilon)} \quad d_B(\mu, \mathcal{M}_{\mathcal{F}}) \leq \delta.$

By monotonicity we can consider $\varepsilon, \delta \in \mathbb{Q}^{+*}$.

Theorem

The SFT $\Omega_{\mathcal{F}}$ is stable iff it satisfies the following formula:

$$\forall \delta \in \mathbb{Q}^{+*}, \exists \varepsilon \in \mathbb{Q}^{+*}, \forall \rho \in \mathbb{Q}^{+*}, \exists \gamma \in \mathbb{Q}^{+*}, \gamma \leq \rho,$$
$$\forall (w, b) \in \widetilde{\mathcal{W}_{\mathcal{F}}^{\varepsilon}}(\gamma), \exists w_0 \in \mathcal{W}_{\mathcal{F}}(\rho), \exists (w_1, w_2) \in (\mathcal{A}^2)^{U_{\psi(\rho, |\mathcal{A}^2|, d)}},$$
$$\left[d^+_{|\mathcal{A}|}\left(\widehat{\delta_{w_1}}, \widehat{\delta_w}\right) < 3\rho\right] \wedge \left[d^+_{|\mathcal{A}|}\left(\widehat{\delta_{w_2}}, \widehat{\delta_{w_0}}\right) < 3\rho\right] \wedge \left[\widehat{\delta_{(w_1, w_2)}}(\Delta) \leq \delta + |\mathcal{A}|^2 \rho\right],$$

with $\widetilde{\mathcal{W}_{\mathcal{F}}^{\varepsilon}}(\gamma)$ and $\mathcal{W}_{\mathcal{F}}(\rho)$ being finite computable sets,
and $U_{\psi(\rho, |\mathcal{A}^2|, d)}$ a computable function.

Hence a Π_4 upper bound on the problem.